



# Lignin oxidation products as a vegetation proxy in stalagmite and drip water samples from the Herbstlabyrinth, Germany

Inken Heidke<sup>1</sup>, Denis Scholz<sup>2</sup>, and Thorsten Hoffmann<sup>1</sup>

<sup>1</sup>Institute of Inorganic Chemistry and Analytical Chemistry, Johannes Gutenberg-University of Mainz, Duesbergweg 10-14, 55128 Mainz, Germany

<sup>2</sup>Institute of Geosciences, Johannes Gutenberg-University of Mainz, J.-J.-Becher-Weg 21, 55128 Mainz, Germany

**Correspondence:** Thorsten Hoffmann (t.hoffmann@uni-mainz.de)

**Abstract.** Here we present the first quantitative record of lignin oxidation products (LOPs) in a Holocene stalagmite from the Herbstlabyrinth Cave in central Germany, as well as LOP results from 16 months of drip water monitoring. Lignin is only produced by vascular plants and is therefore an unambiguous vegetation proxy, which can help to better interpret other vegetation and climate proxies in speleothems. We compared our results with stable isotope and trace element data from the same samples. The drip water monitoring reveals a seasonal pattern of LOPs in a fast drip site with low LOP concentrations in winter and higher LOP concentrations in summer, which is opposite to the behaviour of the drip rate,  $\text{Mg}^{2+}$  and  $\text{PO}_4^{3-}$  concentrations. In the stalagmite, LOP concentrations are correlated or show a similar behaviour to P, Ba and U concentrations. The LOP ratios C/V and S/V, which are usually used to differentiate between angiosperm and gymnosperm and woody and non-woody lignin sources, are anticorrelated to the LOP concentrations and show a similar behaviour to  $\delta^{13}\text{C}$  and Mg concentrations. These results highlight the potential of LOPs as a new, highly specific vegetation proxy in speleothems, but also demonstrate current limitations in our understanding of the transport of lignin from the soil into the cave and the speleothems.

*Copyright statement.*

## 1 Introduction

Speleothems are valuable climate archives, because they can grow continuously for thousands of years and can be dated accurately 500.000 years back in time using the  $^{230}\text{Th}$ -U method (Richards and Dorale, 2003; Scholz and Hoffmann, 2008). Furthermore, the cave provides a preservative environment that protects the recorded chemical proxy signals against outer influences such as light, abrupt changes in temperature and mechanical disturbance. The calcite crystal is able to incorporate and thus preserve not only trace elements and isotopic ratios, but also organic molecules. Until recently, mostly stable isotope ratios and trace elements have been used as climate proxies in speleothems (McDermott, 2004; Fairchild and Treble, 2009). The methodology is well-established, but the records sometimes cannot be interpreted without doubt, unless other proxies are available for comparison (Lachniet, 2009; Fairchild and Treble, 2009; Mischel et al., 2017; Scholz et al., 2012). Therefore, it is important to expand the proxy toolbox of paleoclimate and especially paleo-vegetation reconstruction.



Organic matter in speleothems and cave drip water is most often analyzed as total organic carbon (TOC) or by fluorescence spectroscopy (Quiers et al., 2015). Size exclusion chromatography coupled to organic carbon detection (LC-OCD) was applied to divide organic matter in cave drip water in different fractions, such as biopolymers and humic substances (Rutledge et al., 2015). Only very few molecular organic analytes have been analyzed in speleothems so far. Glycerol dialkyl glycerol tetraethers (GDGTs), which are produced by microorganisms in situ in the cave or the overlying vadose zone, have been implemented as organic temperature proxies (Blyth et al., 2013, 2014). Lipid markers, such as fatty acids (Bosle, 2014) and especially long chain n-alkanes from plant leave waxes, have been used as vegetation proxies, and there have been approaches to use the chain length distribution of n-alkanes to distinguish between the input of grasses and woody plants (Xie, 2003; Blyth et al., 2007, 2011). However, there are uncertainties about the validity of chain length distributions to distinguish between different plant groups (Bush and McInerney, 2013; Blyth et al., 2016). Therefore, a more specific plant biomarker is needed.

Lignin is one of the main constituents of wood and woody plants. It has been widely used as paleo-vegetation proxy in archives such as peat, lake sediments and marine sediment cores (see, for instance, the review by Jex et al., 2014) and as proxy for terrestrial input of plant biomass in natural waters, like rivers and oceans (e.g., Zhang et al., 2013; Standley and Kaplan, 1998; Hernes and Benner, 2002). Blyth and Watson (2009), Blyth et al. (2010) first detected lignin phenols in speleothems, and recently, Heidke et al. (2018) developed a method to quantitatively analyze lignin as a paleo-vegetation proxy in speleothems and cave drip water. The advantage of lignin as a vegetation proxy is that it is only produced by vascular plants and not by microorganisms. Thus, it is very specific. In addition, lignin analysis does not only give information about the abundance, but also about the type of vegetation. The biopolymer lignin consists of three different monomers, coniferyl alcohol, sinapyl alcohol and p-coumaryl alcohol, which are incorporated into the polymer in the form of phenylpropanoids. The proportion of these three monomers varies with the type of vegetation. Lignin from gymnosperm wood consists mainly of coniferyl alcohol, whereas lignin from angiosperm wood contains coniferyl and sinapyl alcohol. Non-woody vegetation, like grasses, leaves and needles, are characterized by a higher proportion of p-coumaryl alcohol. To analyse the lignin composition, the lignin polymer has to be oxidatively degraded into monomeric lignin oxidation products (LOPs). The guaiacyl phenylpropanoid (from coniferyl alcohol) is oxidised to vanillic acid, vanillin and acetovanillone (V-group LOPs), the syringyl phenyl propanoid (from sinapyl alcohol) is oxidised to syringic acid, syringaldehyde and acetosyringone (S-group LOPs), and the p-hydroxyphenyl phenylpropanoid (from p-coumaryl alcohol) is oxidised to p-coumaric acid and ferulic acid (C-group LOPs), but also to p-hydroxybenzoic acid, p-hydroxybenzaldehyde and p-hydroxyacetophenone (H-group LOPs). The latter H-group LOPs can also originate from other sources, like soil microorganisms or the degradation of protein material, and not only from lignin. Therefore, the H-group LOPs are usually not used as vegetation proxies. Usually, the sum parameter  $\Sigma 8$ , which is the sum of all eight individual LOPs from the C-, S- and V-group, is used to present the total lignin concentration. In addition, the ratios of the different LOP groups, C/V and S/V, are used to present the type of lignin, where a higher C/V ratio indicates a higher contribution of non-woody vs. woody plant material and a higher S/V ratio indicates a higher contribution of angiosperm vs. gymnosperm plant material (Hedges and Mann, 1979).

Here, we present the first quantitative record of lignin oxidation products from a Holocene stalagmite from the Herbst-labyrinth in central Germany. In addition, we present LOP results from cave drip water from the same cave, sampled monthly



over a period of 16 months in the framework of a cave monitoring program. The LOP results are compared with stable isotope and trace element records from the same samples recently published by Mischel et al. (2017). This allows to improve our understanding of the processes that affect the transport of lignin into the cave as well as the incorporation into the speleothems.

## 2 Materials and methods

### 5 2.1 The cave monitoring program in the Herbstlabyrinth

From 2010 to 2015, a monthly cave monitoring program, including drip water sampling and the measurement of cave air temperature and  $p\text{CO}_2$  as well as meteorological data, was conducted at the Herbstlabyrinth. A detailed description of the monitoring program, the cave and its environment can be found in Mischel et al. (2015) and Mischel et al. (2017). In brief, the Herbstlabyrinth is situated in the Rhenish Slate Mountains in central Germany. The cave system is about 11 km long and well decorated with different kinds of speleothems. The vegetation above the cave consists of deciduous forest and grassland, and the soil above the cave is a 60 cm-thick Cambisol (Terra fusca). The mean annual temperature at the cave site is  $9.0\text{ }^{\circ}\text{C}$ , and the mean annual precipitation is around  $800\text{ mm} \cdot \text{a}^{-1}$ , with evenly distributed rainfall throughout the year. Due to higher evapotranspiration during summer, the recharge of the aquifer and thus the drip water mainly consists of winter precipitation, but heavy rainfall events in summer can also have a substantial contribution (Mischel et al., 2015). The drip water samples used for lignin analysis were sampled monthly from May 2014 until August 2015. They were collected in precleaned glass vessels from one fast drip site *D1* (average drip rate approx. 0.3–0.5 drops per second), one slow drip site *D2* (average drip rate approx. 60 mL per month) and one cave pool *PW*. To prevent the growth of microorganisms, 5% (w/w) of acetonitrile was added to the samples, which were then stored in the dark at  $4\text{ }^{\circ}\text{C}$  for several months.

### 2.2 The stalagmite sample

Stalagmite NG01 has a light whitish to yellowish colour, is 50 cm long, has a diameter of 15 cm, and grew during the Holocene (Mischel et al., 2017). It was dated via the  $^{230}\text{Th}$ –U method using multicollector-ICP-MS (Mischel et al., 2017). To calculate the age-depth model, the algorithm StalAge was used (Scholz and Hoffmann, 2011). The stalagmite samples used for lignin analysis were cut from a 1 cm thick slab following visible growth lines and had a width along the growth axis of 0.5–2.0 cm, a length of 1.2–4.8 cm and a weight of 2.4–6.2 g. To determine the age and the corresponding error of these samples, the calculated ages for the mid depth and the depth of the upper and lower edges of the sample were used.



## 2.3 Analytical methods

The methods used for dating of the stalagmite samples, the analysis of trace elements and stable isotopes as well as the calculation of the drip rate for the cave drip water samples and the growth rate of the stalagmite are described in detail in Mischel et al. (2017) and references therein. The method used here for the analysis of lignin oxidation products in speleothems and cave drip water is described in detail in Heidke et al. (2018). In the following paragraph, only a brief description will be given. To compare the LOP results with stalagmite data of stable isotopes and trace elements, which have a much higher resolution of 2 mm per sample, a mean value of the higher-resolution data according to the sample size of the LOP samples was calculated. In the discussion, only these lower-resolution data will be shown and discussed. The original data can be found in Mischel et al. (2017). The standard deviations of the respective mean values were used as error bars for the stalagmite stable isotope and trace element data. For the drip water stable isotope and trace element data, the uncertainty is very small and therefore not shown here, but it is provided in Mischel et al. (2017). For the drip water LOP data, the uncertainty was calculated as described in Heidke et al. (2018), and for the stalagmite LOP data, the calculation of the uncertainty is described in section 3.2.

### 2.3.1 Analysis of LOPs

The stalagmite samples were cleaned with organic solvents, edged on the outside with diluted HCl, and finally dissolved in 30% HCl. These sample solutions as well as the drip water samples were extracted via solid phase extraction (SPE), and the extracted lignin was degraded via microwave-assisted CuO oxidation. The resulting lignin oxidation products (LOPs) were again extracted via SPE and then analysed via ultrahigh-performance liquid chromatography (UHPLC) coupled to heated electrospray ionisation (HESI) high resolution mass spectrometry (HRMS) using a Dionex Ultimate 3000 UHPLC system and a Q-Exactive Orbitrap mass spectrometer (Thermo Fisher Scientific). Further details of the method can be found in Heidke et al. (2018).

## 3 Results

### 3.1 LOPs in drip water samples

In Fig. 1, the LOP results of the fast drip site, *D1*, the slow drip site, *D2*, and the cave pool water, *PW*, are shown. The height of the columns represents the sum of the LOP concentrations,  $\Sigma 8$ , and the different colors show the contribution of the C-, S- and V-group LOPs. In general, the V-group LOPs contribute the largest part to the total LOP concentration, followed by the S-group and the C-group LOPs. *D1* shows a strong seasonal pattern with high LOP concentrations between 500 and 1800 ng · L<sup>-1</sup> from May to August 2014 and from April to August 2015, and low LOP concentrations between 30 and 400 ng · L<sup>-1</sup> from September 2014 to February 2015. For July 2014 and March 2015, no data are available. For the slow drip site, *D2*, the concentrations do not show a seasonal pattern, but are highly variable between 80 and 3000 ng · L<sup>-1</sup>. In May, July and August 2014 and June, July and August 2015, there is no data available, mainly because the drip rate was too low to collect a sufficient sample volume.



In the pool water, *PW*, the LOP concentrations show a similar seasonal pattern as in the fast drip site, but less pronounced with concentrations between 140 and 650 ng · L<sup>-1</sup> from September 2014 to February 2015 and between 440 and 1100 ng · L<sup>-1</sup> in the other months, with one exception in April 2015 with more than 2500 ng · L<sup>-1</sup>.

In Fig. 2, the C/V and S/V ratios are shown for *D1*, *D2* and *PW*. Because concentrations of individual analytes were below  
5 the limit of detection, the ratios could not be calculated for every sample. For the different drip sites, the ratios are in a similar range. The ranges of the ratios in *D1* are 0.02–0.33 for C/V, 0.14–1.21 for S/V, . In *D2*, the ranges are 0.00–0.20 for C/V, 0.08–0.68 for S/V, . In *PW*, the ranges are 0.00–0.43 for C/V, 0.18–0.77 for S/V. The ratios of vanillic acid to vanillin (Vac/Val) and syringic acid to syringaldehyde (Sac/Sal) are shown in Fig. S1 in the supplementary information (SI).

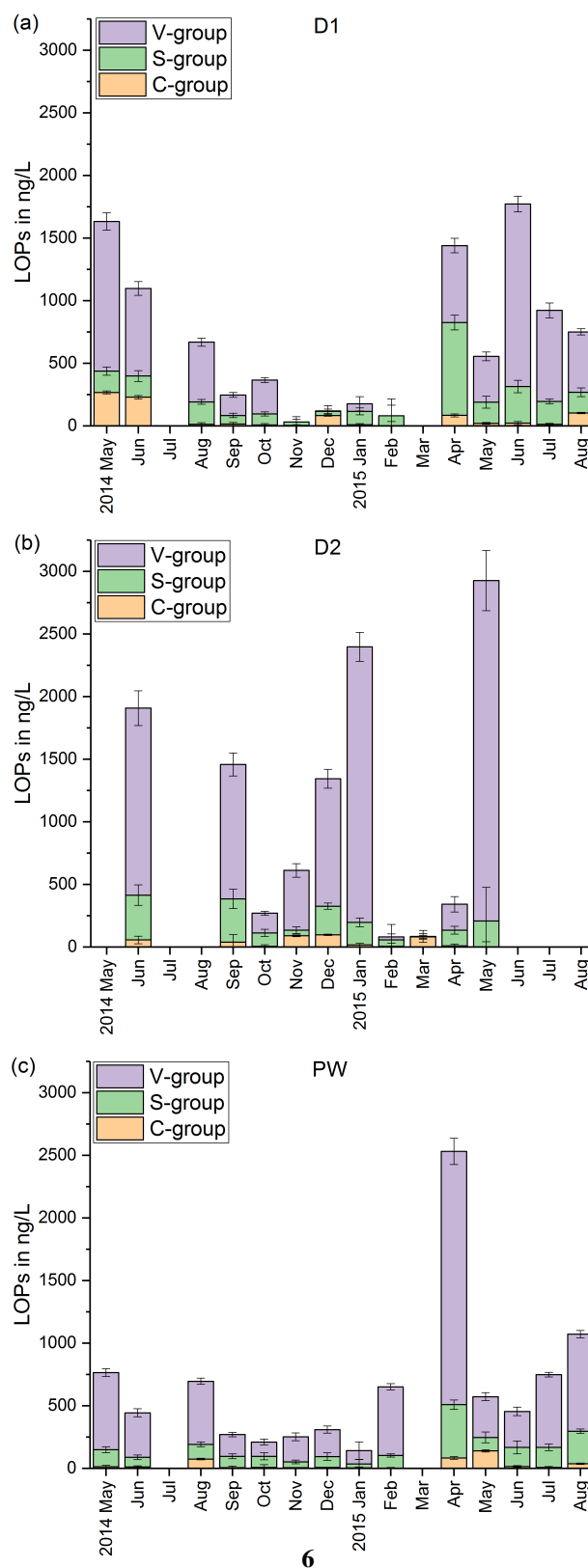


**Figure 1.** LOP results in drip water. (a) fast drip site D1, (b) slow drip site D2, (c) cave pool water.

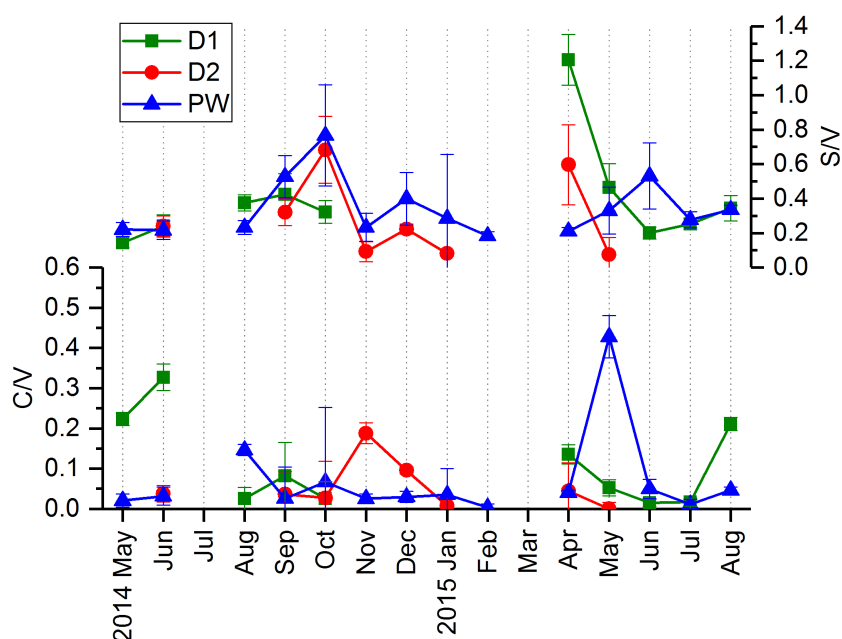


**Figure 2.** C/V and S/V ratios in the drip water.



### 3.2 LOPs in stalagmite samples

One complication of studies with a large number of samples which have to be analyzed over an extended period of time are so-called batch effects, which occur because measurements are affected by laboratory conditions, such as reagent lots, instrumental drift, stability of the reference standards or a varying efficiency of the sample preparation steps (e.g. CuO oxidation step). Since such effects are almost unavoidable, adjustment strategies are generally required (Wehrens et al., 2016; Kirwan et al., 2013; Surowiec et al., 2017), which is especially true when temporal records of the target analytes are the aim of the study. To do so, the stalagmite samples for LOP analysis were analyzed in six batches with nine samples and one blank sample per batch. To recognize systematic errors leading to batch effects, the samples within each batch were not located side by side in the stalagmite, but evenly distributed over the whole length of the stalagmite. In fact, in the results of the LOP concentrations and the C/V and S/V ratios, we observed a regular pattern, which corresponded to the different batches. To uncover the original signal and overcome the differences in instrumental response between the batches, the individual measurements results were revised based on the following correction procedure. In the oldest part of the stalagmite (11.2–8.6 ka BP), the pattern was most visible and least superimposed by original signals. Therefore, we used only this part to calculate a correction factor using equation (1),

$$x_{\text{smoothed}} = x - \bar{X}_{\text{batch } k} + \bar{X}, \quad (1)$$

with  $x_{\text{smoothed}}$  representing the corrected (smoothed) value of  $\Sigma 8$ , C/V or S/V,  $x$  representing the original value of  $\Sigma 8$ , C/V or S/V,  $\bar{X}_{\text{batch } k}$ ,  $k = 1, 2, \dots, 6$ , the mean value of all  $x_i$  in batch  $k$ , and  $\bar{X}$  the mean value of all  $x_i$  of all batches in the oldest part of the stalagmite. The error bars  $\Delta x_{\text{smoothed}}$  for the smoothed values were calculated by equation (2),

$$\Delta x_{\text{smoothed}} = \sqrt{(\Delta x)^2 + (\Delta \bar{X}_{\text{batch } k})^2 + (\Delta \bar{X})^2}, \quad (2)$$

with  $\Delta \bar{X}_{\text{batch } k}$  and  $\Delta \bar{X}$  representing the standard deviations of the respective mean values and  $\Delta x$  representing the uncertainty of a single sample analysis as described in Heidke et al. (2018). The smoothed and original data for  $\Sigma 8$  can be compared in Fig. 3, and for C/V and S/V in Fig. 4.

Figure 3 shows the concentrations of the C-, S- and V-group LOPs as well as the  $\Sigma 8$  concentrations, both smoothed and original data for comparison, plotted against the age of the stalagmite. Figure 4 shows the C/V and S/V ratios, both smoothed and original. The ratios of vanillic acid to vanillin (Vac/Val) and syringic acid to syringaldehyde (Sac/Sal) can be seen in Fig. S2 in the SI (only original data).

The mean  $\Sigma 8$  concentration in the whole stalagmite was  $51 \pm 15 \text{ ng} \cdot \text{g}^{-1}$ . The highest concentrations of up to  $92 \text{ ng} \cdot \text{g}^{-1}$  occurred shortly after the hiatus at the beginning of the middle part at 7.6 ka BP, followed by the lowest concentrations with  $19 \text{ ng} \cdot \text{g}^{-1}$  at 7.0 ka BP. The mean C/V ratio was  $0.32 \pm 0.15$ , with the lowest ratio of 0.12 at 10.9 ka BP and the highest ratios of up to 0.68 at 0.3, 6.5 and 7.2 ka BP. The mean S/V ratio was  $2.15 \pm 0.71$ , with the lowest ratio of 1.08 at 11.1 ka BP and the highest ratios of up to 4.18 at 5.1 and 7.1 ka BP.



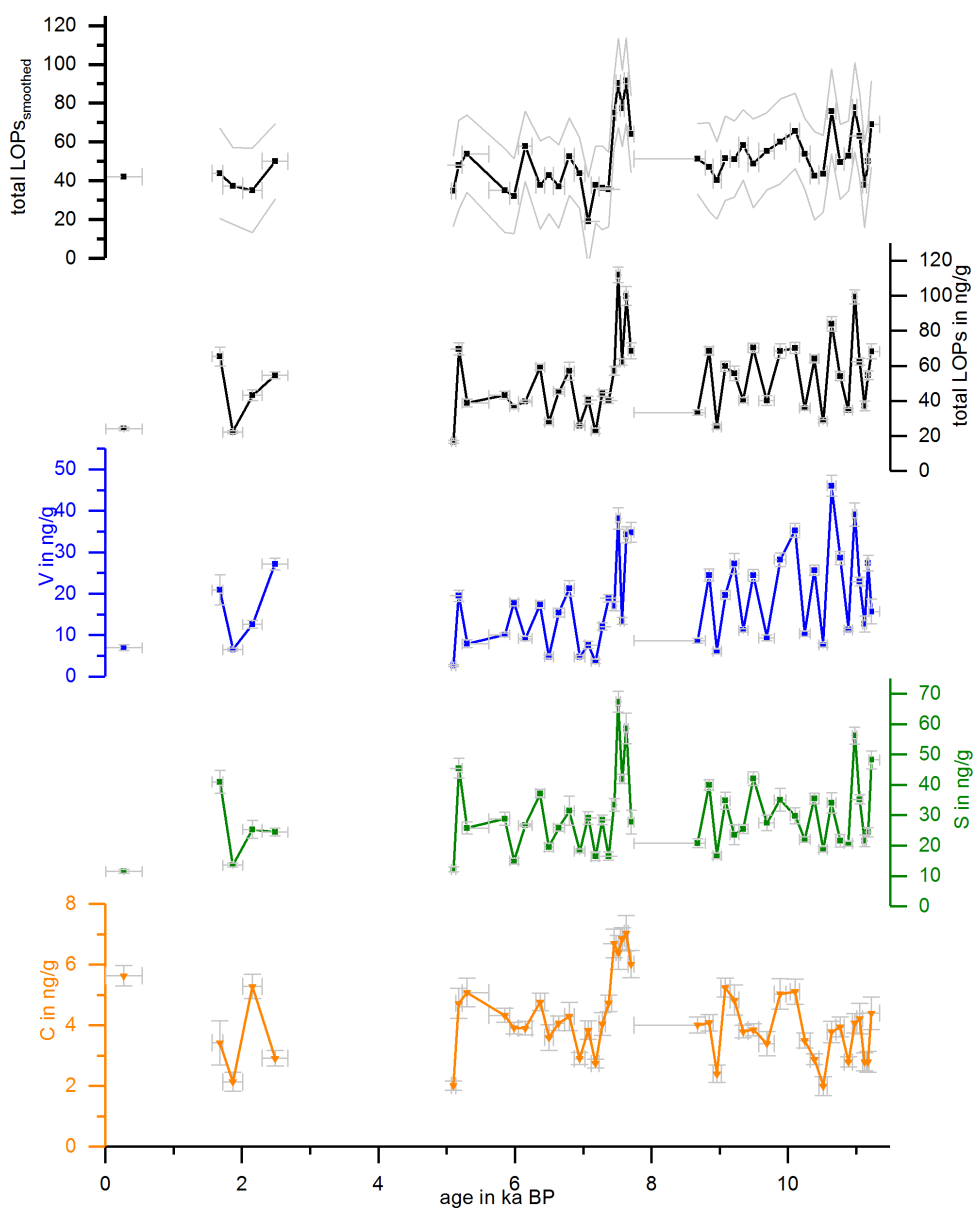


**Figure 3.** Concentrations of the C-, S- and V-group LOPs and  $\Sigma 8$  concentrations plotted against the age of the stalagmite. The uppermost plot shows the smoothed results of  $\Sigma 8$  concentrations.

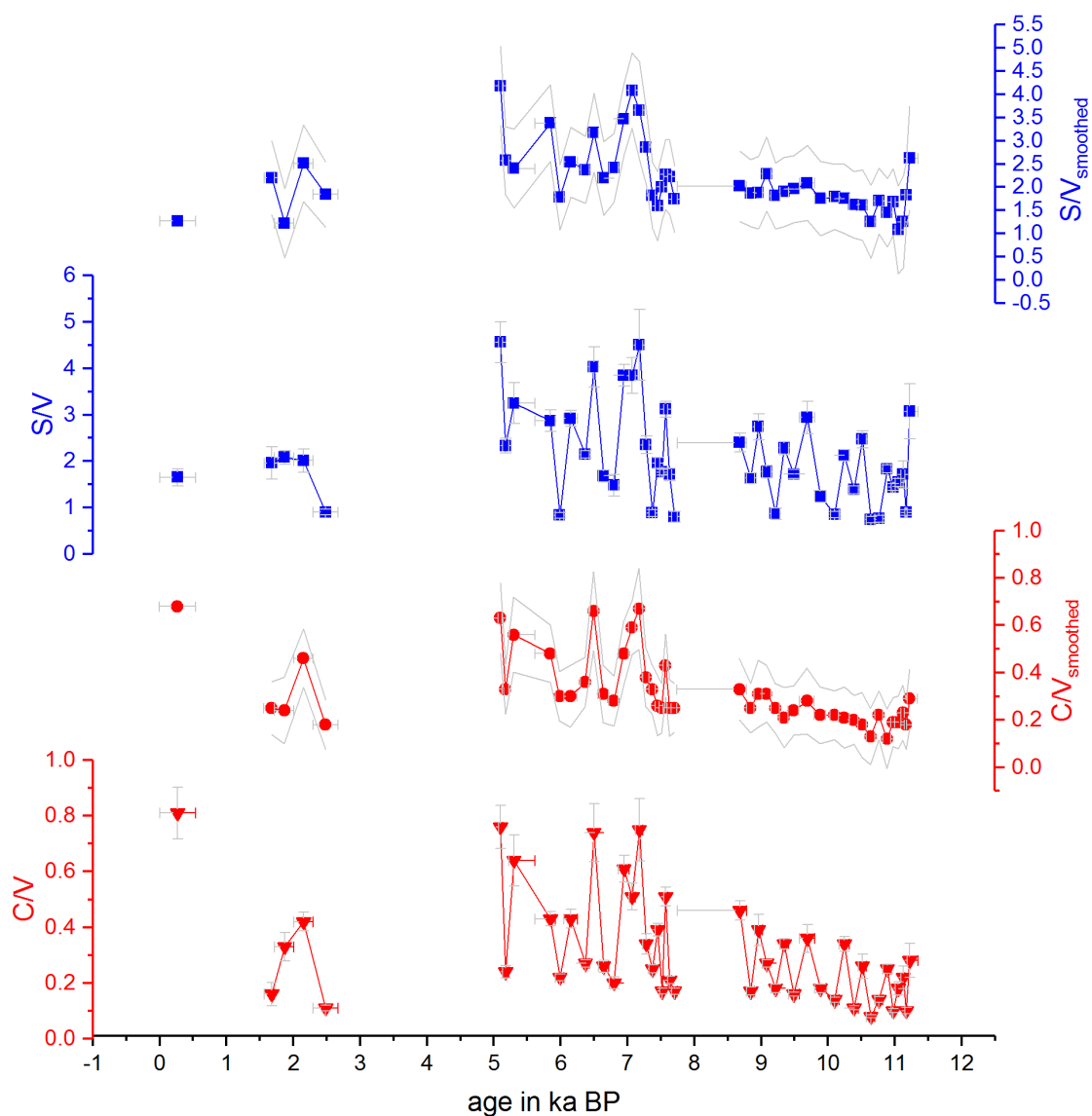


**Figure 4.** Ratios of C/V (red) and S/V (blue), original data and smoothed data, plotted against the age of the stalagmite.



## 4 Discussion

### 4.1 Drip water samples

Figure 5 shows the drip water concentrations of  $\text{Mg}^{2+}$ ,  $\text{PO}_4^{3-}$  and  $\Sigma 8$  as well as the drip rate of the fast drip site *D1*. All three proxies show a strong seasonal pattern here, but with opposite signs.  $\Sigma 8$  concentrations are higher in summer, when the recharge of the aquifer and hence the drip rate are low, and lower in winter, when the recharge and drip rate are high.  $\text{Mg}^{2+}$  and  $\text{PO}_4^{3-}$  concentrations show the opposite behaviour. This is also reflected in a negative correlation of  $\Sigma 8$  and  $\text{Mg}^{2+}$  in *D1*,  $R_{\Sigma 8-\text{Mg}} = -0.67$  ( $p < 0.05$ ). The correlation of  $\Sigma 8$  with  $\text{PO}_4^{3-}$  is not significant at the 95% level, but shows the same tendency,  $R_{\Sigma 8-\text{PO}_4^{3-}} = -0.52$  ( $p = 0.08$ ).

While the sources of lignin are only vascular plants and the source of  $\text{Mg}^{2+}$  is mainly the host rock,  $\text{PO}_4^{3-}$  can originate from both the vegetation and the host rock. Since the seasonal pattern of  $\text{PO}_4^{3-}$  here is similar to that of  $\text{Mg}^{2+}$  and opposed to that of  $\Sigma 8$ , we assume that the  $\text{PO}_4^{3-}$  in the drip water also originates from the hostrock. However, it is important to note that this concerns the seasonal timescale only. At longer timescales, as they are recorded in a stalagmite, the release and mobilization of phosphorous from the hostrock can be related to the productivity of the vegetation above the cave, since phosphorous serves as a plant nutrient.

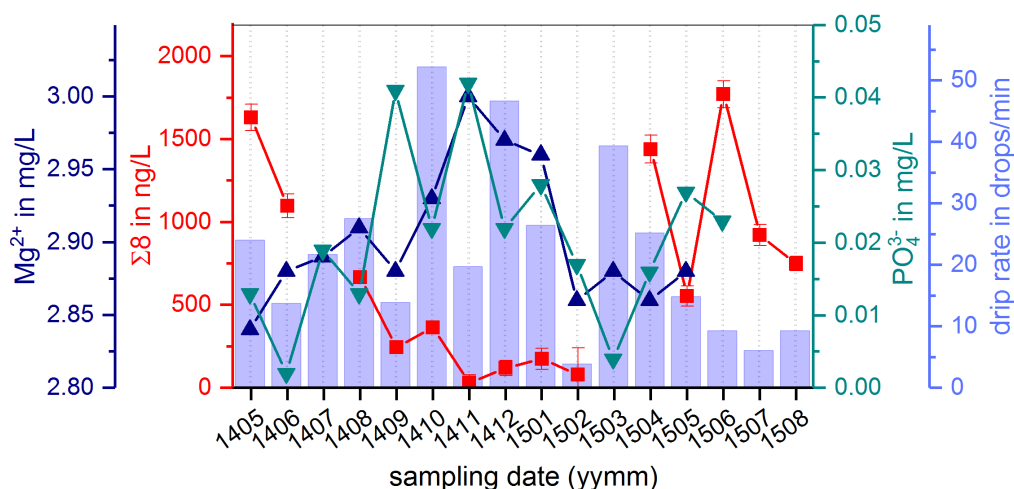


**Figure 5.** Comparison of  $\Sigma 8$  concentrations,  $\text{Mg}^{2+}$ ,  $\text{PO}_4^{3-}$  and drip rate in summer and winter (alternative presentation).

For the LOPs, there might be several causes for the observed concentration pattern. One possible reason could be the growth season of the vegetation from spring to autumn and the activity of soil microorganisms during the warmer time of the year, which would lead to a higher abundance of – partially degraded and therefore transportable – lignin in the soil. However, Mischel et al. (2015) assumed that the drip water of the Herbstlabyrinth is fed by a large reservoir in the karst aquifer, where the water has a residence time of approx. 10 months and is mixed with the water of 12 months. In addition, the degradation



of lignin in the soil takes months to years (Thevenot et al., 2010; Bahri et al., 2006). Therefore, the original seasonality of the input of plant material on the surface will probably be smoothed out by these effects, and it seems more likely that the observed seasonal signal is caused by hydrological effects. A possible reason could be dilution of the – otherwise relatively constant – lignin concentration from the reservoir of organic matter in winter, when the recharge of the aquifer and consequently the drip rate are higher. In summer, in contrast, the slow drip rate and lower recharge of the aquifer might cause a higher concentration of the organic matter and therefore the lignin content in the drip water (Fig. 6).

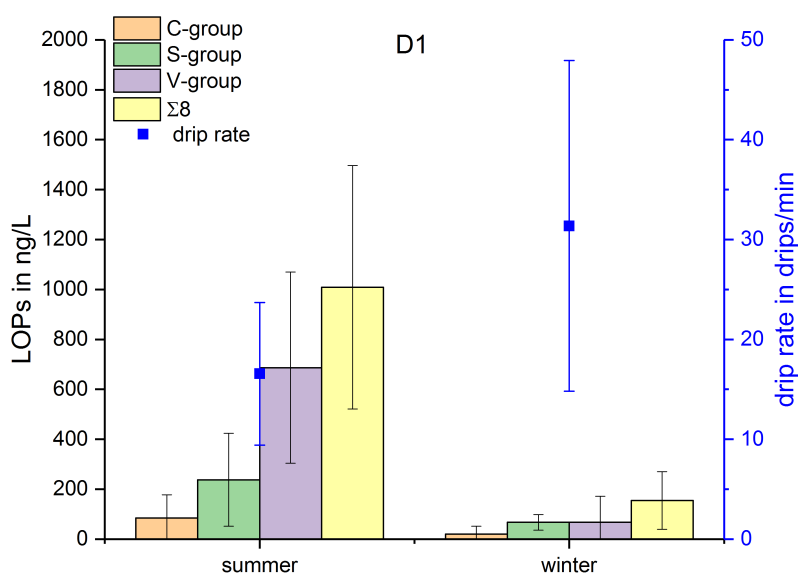


**Figure 6.** Comparison of  $\Sigma 8$  concentrations and drip rate in summer and winter.

A combination of both factors – the activity of the vegetation and the soil microorganisms in summer and the dilution effect due to higher recharge of the aquifer in winter – is also possible to explain the observed seasonal concentration pattern of  $\Sigma 8$ . Interestingly, Bosle (2014), who analyzed low-molecular weight saturated fatty acids as biomarkers for microbial activity in drip water samples from the same cave monitoring program, found a similar seasonal trend with high concentrations during the summer months and low concentrations in winter for the longest fatty acid, arachidic acid ( $C_{20}$ ), but the opposite trend for the shorter chained fatty acids  $C_{12}$  to  $C_{18}$ . Their interpretation was that  $C_{20}$  could be derived from higher plants above the cave, whereas the shorter chained fatty acids could be produced by microorganisms in the cave and the aquifer. This hypothesis seems to be supported by our LOP results.

In Fig. 7, the averaged  $\Sigma 8$  concentrations of the fast drip site, *D1*, the slow drip site, *D2*, and the pool water, *PW*, are compared. On average, the slow drip site *D2* has higher  $\Sigma 8$  concentration than the fast drip site *D1*, and the pool water has the



lowest concentrations. This finding could be explained by dilution effects as discussed above, but also by different reservoirs feeding the different drip sites.

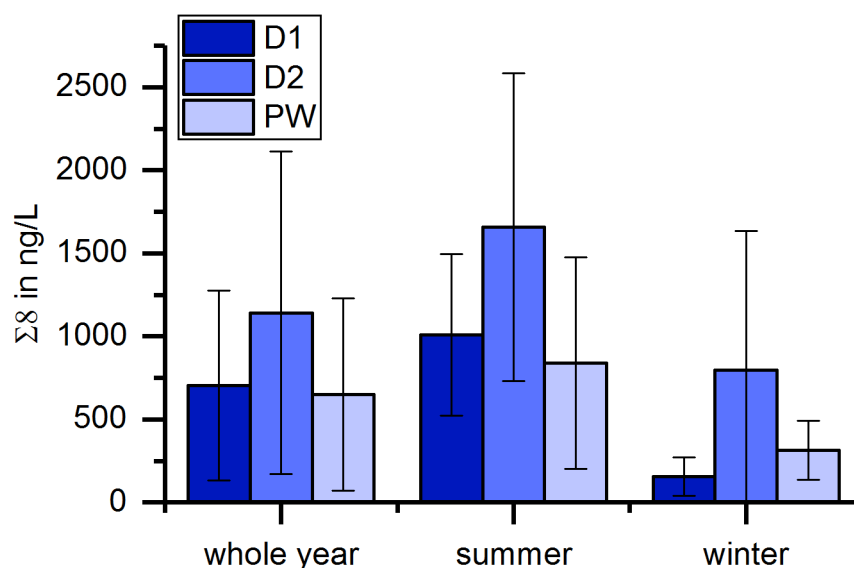


**Figure 7.** Comparison of average  $\Sigma 8$  concentrations of the fast drip site, D1, the slow drip site, D2 and the poolwater, PW.

The interpretation of C/V and S/V in respect to seasonal patterns is rather difficult because there are several data points missing during the winter months where the concentration of the V-group LOPs was below the quantification limit and therefore no C/V or S/V ratios could be calculated. Overall, there is no clear seasonal pattern in the C/V and S/V ratios. On the other hand, we did not expect to see a seasonal pattern here, as the overall vegetation mixture above the cave should stay relatively unchanged throughout one year. Of course, the activity of soil microorganisms can change with temperature and moisture conditions, and the productivity of the vegetation varies over the year. However, if we consider the long turnover times of lignin degradation in soil and assume a reservoir of organic matter above the cave, the C/V and S/V ratios should stay relatively constant. In addition, radiocarbon dating studies showed that the organic matter above caves can be a mix of recent material and material that is up to several hundred years old (Trumbore, 2000; Tegen and Dörr, 1996; Fohlmeister et al., 2011).

The only observable pattern is from 04/2015 to 07/2015, where there was a constant decrease in the C/V and S/V ratios. The same decrease could also be observed in the drip rate, whereas the  $\delta^{13}\text{C}$  values show a constant increase in the same time interval (Fig. 8). The increase in  $\delta^{13}\text{C}$  values could be related to the decreasing drip rate and consequently a longer residence time of the drops in the cave air resulting in increased degassing (Hansen et al., 2017). An explanation for the decrease of C/V and S/V ratios could possibly be linked to the decreasing drip rate, too. In times of reduced recharge of the aquifer, the transport of the lignin from the upper soil into the cave probably takes longer and involves more phase-changes than in times of higher recharge. According to Hernes et al. (2007) and Hernes et al. (2013), every phase-change that occurs to the lignin on



its way from the plant litter to the deeper soil (and into the aquifer and the cave), for example from bound in plant material to dissolved in water and from adsorbed onto mineral surfaces to desorbed, can lead to a fractionation and therefore to a change in the ratios of C/V, S/V and Acid/Aldehyde.

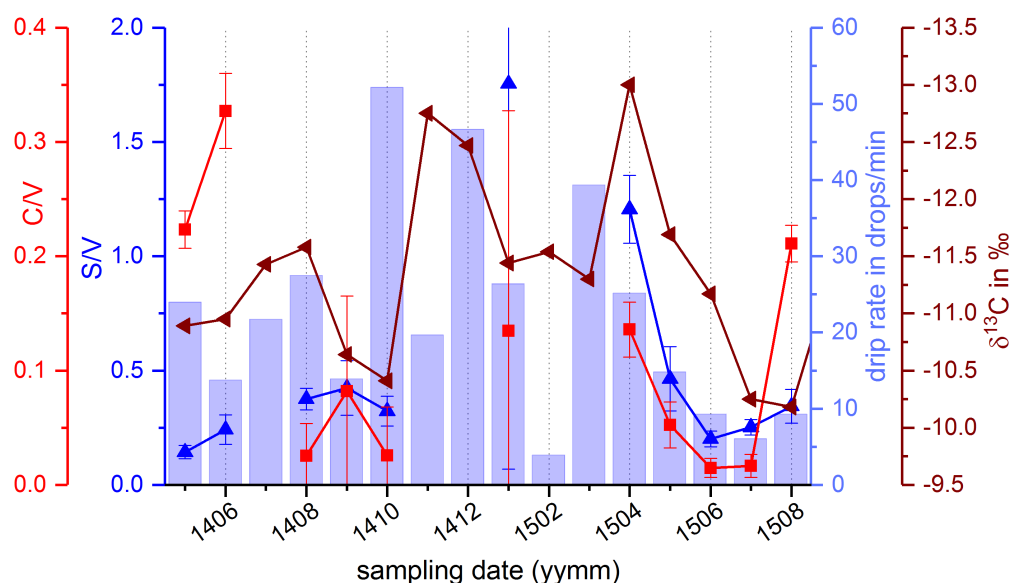


**Figure 8.** Comparison of C/V and S/V ratios with the drip rate and  $\delta^{13}\text{C}$  values in the fast drip site *DI*.

The C/V and S/V ratios of the drip water samples are lower than the ratios found in the stalagmite. This could be interpreted in different ways: Either there was more input of non-woody vegetation or less input of woody vegetation in former times than now, or the difference is also caused by phase-change fractionation as the incorporation into the calcite of the growing speleothem represents a phase-change, too. To find out more about these effects, more comparative studies of LOPs in speleothems and in cave drip water, and, in addition, in situ experiments in an artificial cave (Hansen et al., 2017; Wiedner et al., 2008; Polag et al., 2010) would be beneficial.

## 4.2 Stalagmite samples

In Fig. 9, the lignin parameters  $\Sigma 8$ , C/V and S/V are compared with several trace elements, stable isotopes and the growth rate of the stalagmite. The youngest part of the stalagmite (0–2.5 ka BP) has a lower growth rate and shows a different behaviour of several proxies, e.g. P and  $\delta^{13}\text{C}$ , compared to the rest of the stalagmite. Therefore, Mischel et al. (2017) discussed this part of the stalagmite separately from the two other parts. As the LOP record of the youngest part only consists of five samples, we decided to focus the discussion on the rest of the stalagmite only and did not consider the first five data points for the calculation of correlation coefficients and the principal component analysis. All correlation coefficients for the middle part of

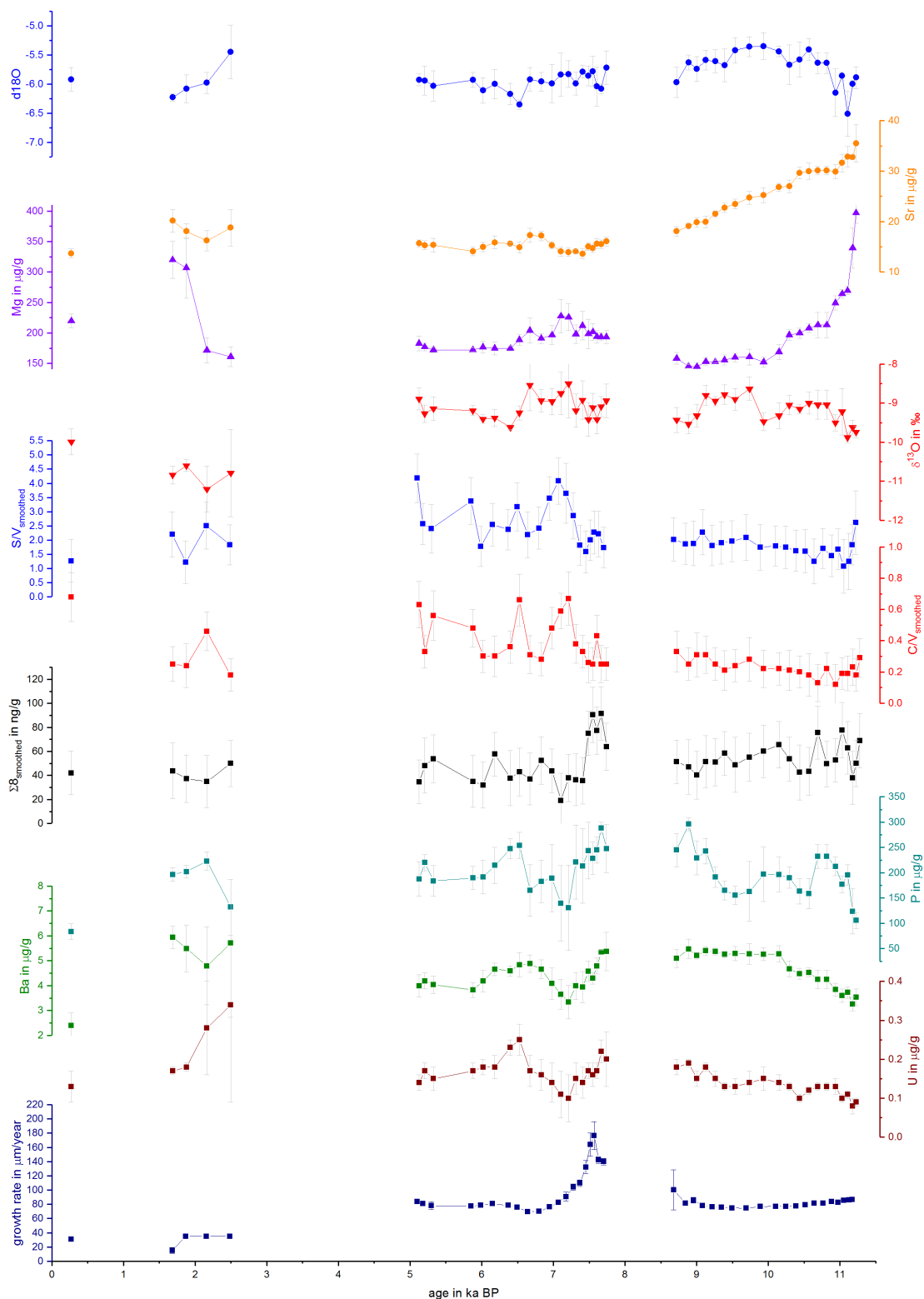


**Figure 9.** Comparison of stable isotopes, trace elements,  $\Sigma 8$  and C/V and S/V ratios, plotted against the age of the stalagmite.



the stalagmite are shown in Table 1, those for the older part are shown in Table S1 in the SI. In contrast to Mischel et al. (2017), we did not detrend the records before calculating the correlations.

The correlation between  $\Sigma 8_{\text{smoothed}}$  and P in the middle part of the stalagmite is  $R_{\Sigma 8-P} = 0.66$  ( $p < 0.01$ ), and the correlation between  $\Sigma 8_{\text{smoothed}}$  and Ba is  $R_{\Sigma 8-Ba} = 0.60$  ( $p < 0.01$ ). This positive correlation between  $\Sigma 8$  and P in the stalagmite is opposite as in the drip water. This shows that the proxy concentrations in the stalagmite and the drip water are influenced by different mechanisms at different timescales. In the older and younger parts of the stalagmite, there are no significant correlations between P or Ba and  $\Sigma 8$ . Uranium shows a similar pattern as P and Ba (Mischel et al., 2017). However, although U is correlated to P and Ba with  $R_{U-P} = 0.79$  and  $R_{U-Ba} = 0.78$ , ( $p < 0.01$ ), there is no significant correlation between U and  $\Sigma 8$ . Mischel et al. (2017) interpreted P, Ba and U as vegetation proxies, with higher concentrations of these elements indicating a more productive vegetation, coinciding with wetter climate conditions. The correlation of  $\Sigma 8$  as an unambiguous vegetation proxy with P, Ba and U confirms this interpretation.

Moreover, there is also a strong positive correlation between  $\Sigma 8$  and the growth rate of the stalagmite,  $R_{\Sigma 8-\text{growth rate}} = 0.79$  ( $p < 0.01$ ). This can be seen especially at the beginning of the middle part (around 8.0–7.5 ka BP, see Fig. 9), where a peak in the growth rate is accompanied by a peak in  $\Sigma 8$  and also in P, Ba, and U concentrations. In the older and younger parts of the stalagmite, there is no such correlation. A higher growth rate can be caused, inter alia, by a higher drip rate or by a higher supersaturation of the drip water with respect to  $\text{CaCO}_3$  (Dreybrodt and Scholz, 2011; Fairchild and Baker, 2012). The latter, in turn, can be caused by a higher soil  $\text{pCO}_2$  due to a more productive vegetation and higher microbial activity in the soil, which would be in accordance with the observed higher concentrations of all vegetation proxies. On the other hand, this peak in the growth rate and the vegetation proxies occurs shortly after a hiatus. Therefore, it is also possible that a change in the flow path of the drip water feeding the stalagmite was responsible for the faster growth of the speleothem and a higher input of organic matter.

The C/V and S/V records have a distinct positive peak at around 7.2 ka BP, and a second, less distinct, positive peak at 6.5 ka BP. Figure 9 shows that at approximately the same time, the concentrations of  $\Sigma 8$  and P are lower or even show negative peaks, indicating less input of organic material. This is also reflected in the negative correlations of C/V and S/V with  $\Sigma 8$  and P in the middle part of the stalagmite,  $R_{\Sigma 8-C/V} = -0.51$  ( $p < 0.05$ ),  $R_{\Sigma 8-S/V} = -0.54$  ( $p < 0.05$ ),  $R_{P-C/V} = -0.48$ , ( $p < 0.05$ ) and  $R_{P-S/V} = -0.53$ , ( $p < 0.05$ ). Furthermore, the records of  $\delta^{13}\text{C}$  and Mg show positive peaks at approximately 7.2 and 6.6 ka BP, although there are no significant correlations of C/V or S/V with  $\delta^{13}\text{C}$  or Mg. Higher concentrations of Mg coinciding with more positive  $\delta^{13}\text{C}$  values in speleothems are often associated with prior calcite precipitation and usually indicate drier conditions (Fairchild and Baker, 2012). Consequently, these peaks can be interpreted as drier periods with less input of organic material. One possible interpretation of the C/V and S/V records is therefore that at drier times with lower lignin input, there was less woody and more non-woody plant material available as a lignin source and the vegetation possibly consisted more of grasses and shrubs. Vice versa, at times with generally higher lignin input, more woody material was the lignin source and the vegetation probably consisted more of forest. Another possible interpretation, which would also be in accordance with the other proxies, would be that during drier conditions in the aquifer, the lignin was transported into the cave





**Table 1.** Correlation coefficients  $R$  for the middle part of the stalagmite.

| middle part                  | C-<br>group | S-<br>group | V-<br>group | C/V<br>smoothed | S/V<br>smoothed | $\Sigma 8$<br>smoothed | Vac/Val | Sac/Sal | $\delta^{13}\text{C}$ | $\delta^{18}\text{O}$ | $^{25}\text{Mg}$ | $^{31}\text{P}$ | $^{88}\text{Sr}$ | $^{137}\text{Ba}$ | $^{238}\text{U}$ |
|------------------------------|-------------|-------------|-------------|-----------------|-----------------|------------------------|---------|---------|-----------------------|-----------------------|------------------|-----------------|------------------|-------------------|------------------|
| C-group                      | 1.00        |             |             |                 |                 |                        |         |         |                       |                       |                  |                 |                  |                   |                  |
| S-group                      | 0.75        | 1.00        |             |                 |                 |                        |         |         |                       |                       |                  |                 |                  |                   |                  |
| V-group                      | 0.74        | 0.72        | 1.00        |                 |                 |                        |         |         |                       |                       |                  |                 |                  |                   |                  |
| C/V <sub>smoothed</sub>      | -0.62       | -0.51       | -0.80       | 1.00            |                 |                        |         |         |                       |                       |                  |                 |                  |                   |                  |
| S/V <sub>smoothed</sub>      | -0.73       | 0           | -0.70       | 0.82            | 1.00            |                        |         |         |                       |                       |                  |                 |                  |                   |                  |
| $\Sigma 8_{\text{smoothed}}$ | 0.81        | 0.75        | 0.66        | -0.51           | -0.54           | 1.00                   |         |         |                       |                       |                  |                 |                  |                   |                  |
| Vac/Val                      | 0.76        | 0.73        | 0           | 0               | 0               | 0.75                   | 1.00    |         |                       |                       |                  |                 |                  |                   |                  |
| Sac/Sal                      | 0.56        | 0.56        | 0           | 0               | 0               | 0.57                   | 0.74    | 1.00    |                       |                       |                  |                 |                  |                   |                  |
| $\delta^{13}\text{C}$        | 0           | 0           | 0           | 0               | 0               | 0                      | 0       | 0       | 1.00                  |                       |                  |                 |                  |                   |                  |
| $\delta^{18}\text{O}$        | 0           | 0           | 0           | 0               | 0               | 0                      | 0       | 0       | 0.52                  | 1.00                  |                  |                 |                  |                   |                  |
| $^{25}\text{Mg}$             | 0           | 0           | 0           | 0               | 0               | 0                      | 0       | 0       | 0.69                  | 0.50                  | 1.00             |                 |                  |                   |                  |
| $^{31}\text{P}$              | 0.67        | 0.52        | 0.55        | -0.48           | -0.53           | 0.66                   | 0.58    | 0       | -0.65                 | 0                     | 0                | 1.00            |                  |                   |                  |
| $^{88}\text{Sr}$             | 0           | 0           | 0           | 0               | 0               | 0                      | 0       | 0       | 0                     | 0                     | 0                | 0               | 1.00             |                   |                  |
| $^{137}\text{Ba}$            | 0.58        | 0           | 0.57        | -0.56           | -0.57           | 0.60                   | 0       | 0       | 0                     | 0                     | 0                | 0.73            | 0.67             | 1.00              |                  |
| $^{238}\text{U}$             | 0           | 0           | 0           | 0               | 0               | 0                      | 0       | 0       | -0.59                 | -0.64                 | -0.55            | 0.80            | 0                | 0.78              | 1.00             |
| growth rate                  | 0.79        | 0.61        | 0.61        | 0               | -0.45           | 0.79                   | 0.62    | 0.56    | 0                     | 0                     | 0                | 0.56            | 0                | 0                 | 0                |



more slowly and therefore had more time to undergo phase-changes on the way, such as adsorption and desorption to mineral surfaces. Such phase-changes can also lead to a change in the C/V and S/V ratios (Hernes et al., 2007).

The pollen-based climate reconstruction from the Meerfelder Maar and the Holzmaar in the Eifel region by Litt et al. (2009) shows a relatively stable vegetation development without any abrupt changes, at least not at the times observed in the C/V and S/V record (6.6 and 7.2 ka BP). This could be interpreted in different ways. One interpretation is that the assumed vegetation changes were local to the region of the the Herbstlabyrinth and did not affect the Eifel region. Another interpretation could be that our proxies are more sensitive to vegetation changes than the pollen record. And third, it is possible that the changes in the vegetation proxies and C/V and S/V were rather caused by changes in the flow paths of the drip water than by changes in the overlaying vegetation. However, Litt et al. (2009) state that their reconstruction method rather underestimates than overestimates climate changes.

In Fig. 10, the principal component analysis of all proxies in the middle and older part of the stalagmite is shown with loadings and scores for the first and second principal components. The first principal component (PC1) explains 31.6% of the overall variance and the second component (PC2) explains 26.9%. Together, these two PCs explain 58.5% of the overall variance. The kink in the scree plot (Fig. S3 in the SI) appears after the fourth PC with PC3 contributing 18.8% and PC4 10.21%, summing up to 87.4% of the variance explained by the first four principal components. However, PC3 and PC4 (Fig. S4 in the SI) are not straightforward to interpret and will not be discussed here. PC1 is composed of Sr and Mg with negative loadings and U, P, Ba, C/V and S/V with positive loadings. It can be inferred from the scores of the individual samples that the influence of Sr and Mg is mainly dominant in the older part of the stalagmite. This long-term decrease of Sr and Mg (see Fig. 9) was interpreted by Mischel et al. (2017) as the result of a thin loess cover, deposited during the last Glacial, being progressively leached at the beginning of the Holocene. PC2 is composed of  $\Sigma 8$ , Ba and P with positive loadings and C/V and S/V with negative loadings. This can be interpreted as the amount of plant organic matter being flushed into the cave.

Overall, we conclude that samples with low lignin content are accompanied by low P, Ba and U concentrations and high C/V and S/V values and vice versa. This confirms P, Ba and U as vegetation proxies, and, in addition, indicates that at times with lower input of organic matter, the composition of the organic matter was different, too. The concurrence of more positive  $\delta^{13}\text{C}$  values and higher Mg concentrations with times of lower vegetational input suggests drier conditions (Mischel et al., 2017), which could have lead to a reduced vegetation cover consisting more of grass than of forest. This highlights the large potential of the lignin proxies for reconstruction of vegetation. However, we cannot say with certainty if the observed changes in the lignin composition result directly from a change in the vegetation cover or from different transport processes in the soil and aquifer. Another example for this ambiguity is the observation that a higher growth rate after the hiatus, at 7.7–7.3 ka BP, is accompanied by higher concentrations of  $\Sigma 8$ , P, Ba and U. This could either indicate a wetter climate with more recharge and a more productive vegetation at that time, or a different flow path of the drip water that lead to both an increased growth rate of the stalagmite and an increased input of organic matter.

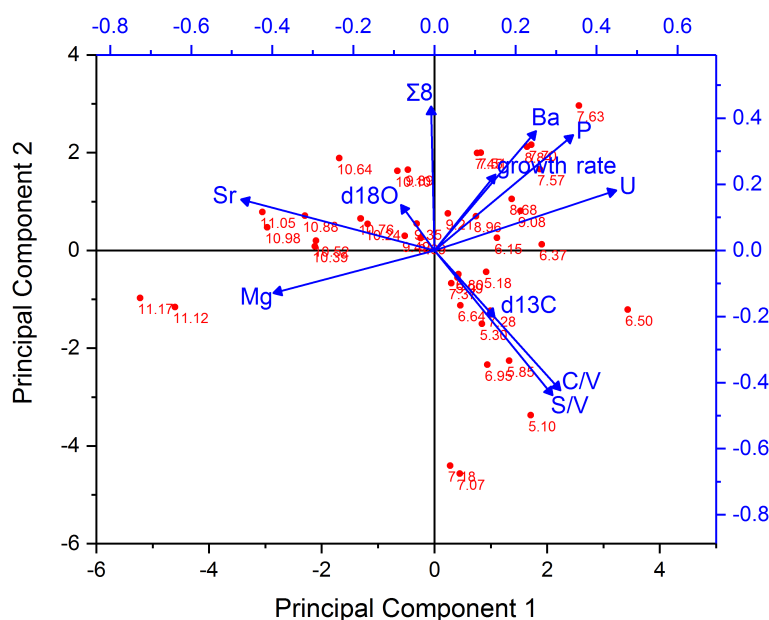


**Figure 10.** Principal component analysis with the variables  $\Sigma 8$ , C/V, S/V, trace elements, growth rate and stable isotopes. The red dots are the scores of the individual samples, labeled with their age in ka BP.

## 5 Conclusions and outlook

The total lignin concentration,  $\Sigma 8$ , seems to be a reliable proxy for the input of plant material into the stalagmites. The  $\Sigma 8$  records fits well with P as an established vegetation proxy for speleothems from the Herbstlabyrinth and also correlates with Ba and U, which also have been interpreted as vegetation proxies by Mischel et al. (2017). The clear benefit of  $\Sigma 8$  compared to these trace elements is, that the sources of lignin are exclusively higher plants and not, for example, microorganisms or the host rock. Therefore,  $\Sigma 8$  can help to better interpret potential vegetation proxies whose sources are less clear.

The interpretation of the lignin parameters C/V and S/V seems to be more complicated, as these ratios might be influenced not only by the type of the overlying vegetation, but also by phase-change fractionation due to adsorption and desorption processes on the way from the soil into the cave, which can differ for different flow paths. Greater changes in the vegetation, such as longer periods of deforestation, will probably still cause changes in the C/V and S/V ratios, but more research is needed to understand all possible influences.

In future studies, more speleothem samples from different vegetation and climate zones should be analyzed to study the relation of vegetation types above the cave and LOP ratios found in the speleothems. To get more insight into possible fractionation processes occurring on the way from the soil to the cave, comparative studies of LOPs in soil, drip water and speleothems



should be carried out. In addition to stalagmites, flowstones could be valuable sample material because they are often fed by water flows with higher discharge carrying larger amounts of organic material.

*Data availability.* We have provided all relevant data in the paper and the supplement to this study.

*Author contributions.* IH, DS, and TH designed the research; IH performed the research; IH, DS, and TH analyzed the data and all authors  
5 contributed to writing the paper

*Competing interests.* The authors declare that they have no conflict of interest.

*Disclaimer.*

*Acknowledgements.* We thank Simon Mischel for providing stalagmite and cave drip water samples from the Herbstlabyrinth Cave. This project has received funding from the European Union's Horizon 2020 research and innovation program under Marie Skłodowska-Curie  
10 grant agreement no. 691037. Denis Scholz acknowledges funding from the German Research Foundation (SCHO 1274/3-1 and SCHO 1274/9-1).



## References

- Bahri, H., Dignac, M.-F., Rumpel, C., Rasse, D. P., Chenu, C., and Mariotti, A.: Lignin turnover kinetics in an agricultural soil is monomer specific, *Soil Biology and Biochemistry*, 38, 1977–1988, 2006.
- Blyth, A. J. and Watson, J. S.: Thermochemolysis of organic matter preserved in stalagmites: A preliminary study, *Organic Geochemistry*, 40, 1029–1031, 2009.
- Blyth, A. J., Asrat, A., Baker, A., Gulliver, P., Leng, M. J., and Genty, D.: A new approach to detecting vegetation and land-use Change using high-resolution lipid biomarker records in stalagmites, *Quaternary Research*, 68, 314–324, 2007.
- Blyth, A. J., Watson, J. S., Woodhead, J., and Hellstrom, J.: Organic compounds preserved in a 2.9million year old stalagmite from the Nullarbor Plain, Australia, *Chemical Geology*, 279, 101–105, 2010.
- Blyth, A. J., Baker, A., Thomas, L. E., and van Calsteren, P.: A 2000-year lipid biomarker record preserved in a stalagmite from north-west Scotland, *Journal of Quaternary Science*, 26, 326–334, 2011.
- Blyth, A. J., Shutova, Y., and Smith, C.:  $\delta^{13}\text{C}$  analysis of bulk organic matter in speleothems using liquid chromatography–isotope ratio mass spectrometry, *Organic Geochemistry*, 55, 22–25, 2013.
- Blyth, A. J., Jex, C. N., Baker, A., Khan, S. J., and Schouten, S.: Contrasting distributions of glycerol dialkyl glycerol tetraethers (GDGTs) in speleothems and associated soils, *Organic Geochemistry*, 69, 1–10, 2014.
- Blyth, A. J., Hartland, A., and Baker, A.: Organic proxies in speleothems – New developments, advantages and limitations, *Quaternary Science Reviews*, 149, 1–17, 2016.
- Bosle, J. M.: Dissertation: Methodenentwicklung zur Spurenanalyse organischer Biomarker in Speläothemen und Tropfwasser mittels Flüssigchromatographie-(HR-)Massenspektrometrie, 2014.
- Bush, R. T. and McInerney, F. A.: Leaf wax n-alkane distributions in and across modern plants: Implications for paleoecology and chemotaxonomy, *Geochimica et Cosmochimica Acta*, 117, 161–179, 2013.
- Dreybrodt, W. and Scholz, D.: Climatic dependence of stable carbon and oxygen isotope signals recorded in speleothems: From soil water to speleothem calcite, *Geochimica et Cosmochimica Acta*, 75, 734–752, 2011.
- Fairchild, I. J. and Baker, A.: *Speleothem Science*, John Wiley & Sons, Ltd, Chichester, UK, 2012.
- Fairchild, I. J. and Treble, P. C.: Trace elements in speleothems as recorders of environmental change, *Quaternary Science Reviews*, 28, 449–468, 2009.
- Fohlmeister, J., Kromer, B., and Mangini, A.: The Influence of Soil Organic Matter Age Spectrum on the Reconstruction of Atmospheric  $^{14}\text{C}$  Levels Via Stalagmites, *Radiocarbon*, 53, 99–115, 2011.
- Hansen, M., Scholz, D., Froeschmann, M.-L., Schöne, B. R., and Spötl, C.: Carbon isotope exchange between gaseous  $\text{CO}_2$  and thin solution films: Artificial cave experiments and a complete diffusion-reaction model, *Geochimica et Cosmochimica Acta*, 211, 28–47, 2017.
- Hedges, J. I. and Mann, D. C.: The characterization of plant tissues by their lignin oxidation products, *Geochimica et Cosmochimica Acta*, 43, 1803–1807, 1979.
- Heidke, I., Scholz, D., and Hoffmann, T.: Quantification of lignin oxidation products as vegetation biomarkers in speleothems and cave drip water, *Biogeosciences*, 15, 5831–5845, 2018.
- Hernes, P. J. and Benner, R.: Transport and diagenesis of dissolved and particulate terrigenous organic matter in the North Pacific Ocean, *Deep Sea Research Part I: Oceanographic Research Papers*, 49, 2119–2132, <http://www.sciencedirect.com/science/article/pii/S0967063702001280>, 2002.



- Hernes, P. J., Robinson, A. C., and Aufdenkampe, A. K.: Fractionation of lignin during leaching and sorption and implications for organic matter “freshness”, *Geophysical Research Letters*, 34, 1921, 2007.
- Hernes, P. J., Kaiser, K., Dyda, R. Y., and Cerli, C.: Molecular trickery in soil organic matter: hidden lignin, *Environmental science & technology*, 47, 9077–9085, 2013.
- 5 Jex, C. N., Pate, G. H., Blyth, A. J., Spencer, R. G., Hernes, P. J., Khan, S. J., and Baker, A.: Lignin biogeochemistry: from modern processes to Quaternary archives, *Quaternary Science Reviews*, 87, 46–59, 2014.
- Kirwan, J. A., Broadhurst, D. I., Davidson, R. L., and Viant, M. R.: Characterising and correcting batch variation in an automated direct infusion mass spectrometry (DIMS) metabolomics workflow, *Analytical and bioanalytical chemistry*, 405, 5147–5157, 2013.
- Lachniet, M. S.: Climatic and environmental controls on speleothem oxygen-isotope values, *Quaternary Science Reviews*, 28, 412–432, 10 2009.
- Litt, T., Schölzel, C., Kühl, N., and Brauer, A.: Vegetation and climate history in the Westeifel Volcanic Field (Germany) during the past 11 000 years based on annually laminated lacustrine maar sediments, *Boreas*, 38, 679–690, 2009.
- McDermott, F.: Palaeo-climate reconstruction from stable isotope variations in speleothems: a review, *Quaternary Science Reviews*, 23, 901–918, 2004.
- 15 Mischel, S. A., Scholz, D., and Spötl, C.:  $\delta^{18}\text{O}$  values of cave drip water: a promising proxy for the reconstruction of the North Atlantic Oscillation?, *Climate Dynamics*, 45, 3035–3050, 2015.
- Mischel, S. A., Scholz, D., Spötl, C., Jochum, K. P., Schröder-Ritzrau, A., and Fiedler, S.: Holocene climate variability in Central Germany and a potential link to the polar North Atlantic: A replicated record from three coeval speleothems, *The Holocene*, 27, 509–525, 2017.
- Polag, D., Scholz, D., Mühlinghaus, C., Spötl, C., Schröder-Ritzrau, A., Segl, M., and Mangini, A.: Stable isotope fractionation in 20 speleothems: Laboratory experiments, *Chemical Geology*, 279, 31–39, 2010.
- Quiers, M., Perrette, Y., Chalmin, E., Fanget, B., and Poulenard, J.: Geochemical mapping of organic carbon in stalagmites using liquid-phase and solid-phase fluorescence, *Chemical Geology*, 411, 240–247, <http://www.sciencedirect.com/science/article/pii/S0009254115003319>, 2015.
- Richards, D. A. and Dorale, J. A.: Uranium-series Chronology and Environmental Applications of Speleothems, *Reviews in Mineralogy and 25 Geochemistry*, 52, 407–460, 2003.
- Rutledge, H., Andersen, M. S., Baker, A., Chinu, K. J., Cuthbert, M. O., Jex, C. N., Marjo, C. E., Markowska, M., and Rau, G. C.: Organic characterisation of cave drip water by LC-OCD and fluorescence analysis, *Geochimica et Cosmochimica Acta*, 166, 15–28, <http://www.sciencedirect.com/science/article/pii/S0016703715003671>, 2015.
- Scholz, D. and Hoffmann, D.:  $^{230}\text{Th}/\text{U}$ -dating of fossil corals and speleothems, *Quat. Sci. J.*, 57, 52–76, 2008.
- 30 Scholz, D. and Hoffmann, D. L.: StalAge – An algorithm designed for construction of speleothem age models, *Quaternary Geochronology*, 6, 369–382, 2011.
- Scholz, D., Frisia, S., Borsato, A., Spötl, C., Fohlmeister, J., Mudelsee, M., Miorandi, R., and Mangini, A.: Holocene climate variability in north-eastern Italy: potential influence of the NAO and solar activity recorded by speleothem data, *Climate of the Past*, 8, 1367–1383, 2012.
- 35 Standley, L. J. and Kaplan, L. A.: Isolation and analysis of lignin-derived phenols in aquatic humic substances: improvements on the procedures, *Organic Geochemistry*, 28, 689–697, <http://www.sciencedirect.com/science/article/pii/S0146638098000412>, 1998.



- Surowiec, I., Johansson, E., Torell, F., Idborg, H., Gunnarsson, I., Svenungsson, E., Jakobsson, P.-J., and Trygg, J.: Multivariate strategy for the sample selection and integration of multi-batch data in metabolomics, *Metabolomics : Official journal of the Metabolomic Society*, 13, 114, 2017.
- Tegen, I. and Dörr, H.:  $^{14}\text{C}$  Measurements of Soil Organic Matter, Soil  $\text{CO}_2$  and Dissolved Organic Carbon (1987–1992), *Radiocarbon*, 38, 247–251, 1996.
- Thevenot, M., Dignac, M.-F., and Rumpel, C.: Fate of lignins in soils: A review, *Soil Biology and Biochemistry*, 42, 1200–1211, 2010.
- Trumbore, S.: Age of soil organic matter and soil respiration: radiocarbon constraints on belowground C dynamics, *Ecological Applications*, 10, 399–411, 2000.
- Wehrens, R., Hageman, J. A., van Eeuwijk, F., Kooke, R., Flood, P. J., Wijnker, E., Keurentjes, J. J. B., Lommen, A., van Eekelen, H. D. L. M., Hall, R. D., Mumm, R., and de Vos, R. C. H.: Improved batch correction in untargeted MS-based metabolomics, *Metabolomics : Official journal of the Metabolomic Society*, 12, 88, 2016.
- Wiedner, E., Scholz, D., Mangini, A., Polag, D., Mühlinghaus, C., and Segl, M.: Investigation of the stable isotope fractionation in speleothems with laboratory experiments, *Quaternary International*, 187, 15–24, 2008.
- Xie, S.: Lipid distribution in a subtropical southern China stalagmite as a record of soil ecosystem response to paleoclimate change, *Quaternary Research*, 2003.
- Zhang, T., Li, X., Sun, S., Lan, H., Du, P., and Wang, M.: Determination of lignin in marine sediment using alkaline cupric oxide oxidation-solid phase extraction-on-column derivatization-gas chromatography, *Journal of Ocean University of China*, 12, 63–69, 2013.